



**HAL**  
open science

## Tracing solar wind plasma entry into the magnetosphere using ion-to-electron temperature ratio

B. Lavraud, J. E. Borovsky, Vincent Génot, S. J. Schwartz, J. Birn, A. N. Fazakerley, M. W. Dunlop, M. G. G. T. Taylor, H. Hasegawa, A. P. Rouillard,  
et al.

► **To cite this version:**

B. Lavraud, J. E. Borovsky, Vincent Génot, S. J. Schwartz, J. Birn, et al.. Tracing solar wind plasma entry into the magnetosphere using ion-to-electron temperature ratio. 2009. hal-00422150

**HAL Id: hal-00422150**

**<https://hal.science/hal-00422150>**

Preprint submitted on 6 Oct 2009

**HAL** is a multi-disciplinary open access archive for the deposit and dissemination of scientific research documents, whether they are published or not. The documents may come from teaching and research institutions in France or abroad, or from public or private research centers.

L'archive ouverte pluridisciplinaire **HAL**, est destinée au dépôt et à la diffusion de documents scientifiques de niveau recherche, publiés ou non, émanant des établissements d'enseignement et de recherche français ou étrangers, des laboratoires publics ou privés.

# 1 Tracing solar wind plasma entry into the magnetosphere 2 using ion-to-electron temperature ratio

3 B. Lavraud,<sup>1,2</sup> J. E. Borovsky,<sup>3</sup> V. Génot,<sup>1,2</sup> S. J. Schwartz,<sup>4</sup> J. Birn,<sup>3</sup> A. N.  
4 Fazakerley,<sup>5</sup> M. W. Dunlop,<sup>6</sup> M. G. G. T. Taylor,<sup>7</sup> H. Hasegawa,<sup>8</sup> A. P.  
5 Rouillard,<sup>6</sup> J. Berchem,<sup>9</sup> Y. Bogdanova,<sup>10</sup> D. Constantinescu,<sup>11</sup> I. Dandouras,<sup>1,2</sup>  
6 J. P. Eastwood,<sup>12</sup> C. P. Escoubet,<sup>7</sup> H. Frey,<sup>12</sup> C. Jacquey,<sup>1,2</sup> E. Panov,<sup>13</sup> Z. Y.  
7 Pu,<sup>14</sup> C. Shen,<sup>15</sup> J. Shi,<sup>15</sup> D. G. Sibeck,<sup>16</sup> M. Volwerk,<sup>13</sup> and J. A. Wild,<sup>17</sup>

8  
9 <sup>1</sup> Centre d'Etude Spatiale des Rayonnements, Université de Toulouse (UPS), France

10 <sup>2</sup> Centre National de la Recherche Scientifique, UMR 5187, Toulouse, France

11 <sup>3</sup> Space Science and Applications, Los Alamos National Laboratory, USA

12 <sup>4</sup> The Blackett Laboratory, Imperial College, London, UK

13 <sup>5</sup> Mullard Space Science Laboratory, Dorking, UK

14 <sup>6</sup> Rutherford Appleton Laboratory, Didcot, UK

15 <sup>7</sup> ESTEC/ESA, Noordwijk, The Netherlands

16 <sup>8</sup> Institute of Space and Astronautical Science, JAXA, Sagami-hara, Japan

17 <sup>9</sup> IGPP/UCLA, Los Angeles, USA

18 <sup>10</sup> Department of Physics, La Trobe University, Victoria, Australia

19 <sup>11</sup> Geophysik & extraterrestrische Physik, Braunschweig, Germany

20 <sup>12</sup> Space Sciences Laboratory, UC Berkeley, USA

21 <sup>13</sup> Space Research Institute, Graz, Austria

22 <sup>14</sup> School of Earth and Space Sciences, Beijing, China

23 <sup>15</sup> Center for Space Science and Applied Research, Beijing, China

24 <sup>16</sup> NASA/GSFC, Greenbelt, USA

25 <sup>17</sup> Department of Communication Systems, Lancaster Univ., UK

26 **Abstract.** When the solar wind Mach number is low, typically such as in magnetic clouds,  
27 the physics of the bow shock leads to a downstream ion-to-electron temperature ratio that can  
28 be notably lower than usual. We utilize this property to trace solar wind plasma entry into the  
29 magnetosphere by use of Cluster measurements in the vicinity of the dusk magnetopause  
30 during the passage of a magnetic cloud at Earth on November 25, 2001. The ion-to-electron  
31 temperature ratio was indeed low in the magnetosheath ( $T_i/T_e \sim 3$ ). In total, three  
32 magnetopause boundary layer intervals are encountered on that day. They all show that the  
33 low ion-to-electron temperature ratio [can be preserved](#) as the plasma enters the  
34 magnetosphere, and both with and without the observation of Kelvin-Helmholtz activity. This  
35 suggests that the ion-to-electron temperature ratio in the magnetopause boundary layer, which  
36 is usually high, is not prescribed by the heating characteristics of the plasma entry mechanism  
37 that formed these boundary layers. In the future, this property may be used to (1) further trace  
38 plasma entry into inner regions and (2) determine the preferred entry mechanisms if other  
39 theoretical, observational and simulation works can give indications on which mechanisms  
40 may alter this ratio.

## 41 1. Introduction

42 The solar wind is decelerated and diverted at the bow  
43 shock that forms upstream of the Earth's magnetosphere.  
44 The bow shock creates a denser and hotter plasma region  
45 that engulfs the magnetosphere: the magnetosheath. It is  
46 not the pristine solar wind, but rather the processed  
47 magnetosheath plasma, that interacts with the  
48 magnetosphere at the magnetopause. Accurate knowledge  
49 of the characteristics of the magnetosheath is thus crucial.  
50 In particular, its specific properties during low Alfvén  
51 Mach number ( $M_A$ ) drastically alter solar wind –  
52 magnetosphere coupling, as described by *Lavraud and*  
53 *Borovsky* [2008].

54 For typical solar wind conditions, i.e., high  $M_A$  ( $> 6$ ),  
55 energy conversion at the bow shock leads to high ion-to-  
56 electron ( $T_i/T_e$ ) temperature ratio. From earlier works on  
57 the magnetosheath close to the dayside magnetopause,  
58  $T_i/T_e$  appears variable and statistically in the range 6 – 12

59 [Paschmann *et al.*, 1993; Phan *et al.*, 1994]. At lower  $M_A$ ,  
60 bow shock properties change. In addition to the decreased  
61 compression ratio ( $< 4$ ), which affects the downstream  
62 magnetosheath densities and magnetic field, lower  $M_A$   
63 leads to lower downstream  $T_i/T_e$ . Although with  
64 significant scatter in the datasets studied, this trend has  
65 been well established [e.g., Bame *et al.*, 1979; Russell *et*  
66 *al.*, 1982; Thomsen *et al.*, 1985; Schwartz *et al.*, 1988].

67 With significant scatter as well, the Earth's central  
68 plasma sheet and plasma sheet boundary layers have  
69 average  $T_i/T_e \sim 7$  [Baumjohann, 1993], thus comparable to  
70 that in the magnetosheath. The magnetopause boundary  
71 layers, inside and directly attached to the magnetopause,  
72 contain heated ions and electrons of solar wind origin that  
73 have entered the magnetosphere [e.g., Eastman and  
74 Hones, 1979; Mitchell *et al.*, 1987]. The main processes  
75 that have been invoked for their formation are related to  
76 magnetic reconnection, diffusive entry and the Kelvin-  
77 Helmholtz (KH) instability [e.g., Dungey, 1961; Song and  
78 Russell, 1992; Lee *et al.*, 1994; Terasawa *et al.*, 1997;  
79 Fujimoto *et al.*, 1998; Sibeck *et al.*, 1999; Hasegawa *et al.*,  
80 2004; Nykyri *et al.*, 2006; Lavraud *et al.*, 2006]. A  
81 question that naturally arises is whether  $T_i/T_e$  in the  
82 plasma sheet and boundary layers is set (1) by the heating  
83 properties of the plasma entry processes or (2) simply by  
84 the temperature ratio of the source magnetosheath, if this  
85 ratio is preserved as magnetosheath plasma enters the  
86 magnetosphere.

87 In this paper, we study a Cluster encounter with the  
88 dusk side magnetopause during the passage of a low  $M_A$   
89 magnetic cloud. It demonstrates that a low ion-to-electron  
90 temperature ratio may indeed be preserved upon entry into  
91 the boundary layers.

## 92 2. Instrumentation

93 We utilize data from the ion (CIS/HIA; Rème *et al.*  
94 [2001]), electron (PEACE; Johnstone *et al.* [1997]), and  
95 magnetic field (FGM; Balogh *et al.* [2001]) instruments  
96 onboard Cluster spacecraft 1. We use 4 s onboard ion and  
97 electron moments. Electron moments were corrected for  
98 the spacecraft potential and energy cutoffs as explained in  
99 Génot and Schwartz [2004]; they are consistent with the  
100 lower resolution on-ground moments. We also use OMNI  
101 solar wind data (from the ACE spacecraft) to provide the  
102 context of Cluster observations. Only GSM coordinates  
103 are used.

## 104 3. Observations

105 Figure 1 shows the solar wind context of the Cluster  
106 observations. A magnetic cloud passed by Earth between  
107 14 UT on November 24 and 11 UT on November 26, 2001  
108 (blue horizontal arrow). It was preceded by a strong shock  
109 and an extended sheath region with large dynamic  
110 pressure (Figure 1b). The magnetic field in the sheath was  
111 fluctuating and strong, leading to an intense geomagnetic  
112 storm ( $Dst < -200$  nT; not shown). The magnetic cloud  
113 had a very high speed (Figure 1c), explaining the strong  
114 compression ahead of it. The leading portion of the core of  
115 the magnetic cloud was less geoeffective since it had a less  
116 intense and northward magnetic field. The magnetic cloud  
117 is characterized by a strong magnetic field but a density

118 significantly lower than the sheath; consequently  $M_A$  was  
119 low ( $\sim 2$ -5; Figure 1d).

120 Cluster instrumentation was only operational during the  
121 interval delimited by the vertical dashed lines in Figure 1,  
122 i.e., when  $M_A$  was low. For reference, Cluster location was  
123 (-3.4, 18.0, -5.2) Earth Radii (GSM) around 09 UT on  
124 November 25, i.e., on the dusk-side southern flank just  
125 tailward of the dawn-dusk terminator. As will be obvious  
126 later from the data, Cluster was always located near the  
127 dusk magnetopause, moving from north to south across  
128 the equatorial plane near its apogee.

129 The top panels of Figure 2 show Cluster data for the  
130 interval of operation. The spacecraft first observed wave  
131 activity, which we analyse in more detail later. Around  
132 03:30 UT, the spacecraft entered the magnetosheath,  
133 characterized by larger tailward flow, higher density and  
134 northward magnetic field (panels (e), (b), and (f)). The low  
135 density (a few  $\text{cm}^{-3}$ , a result of the low  $M_A$ ) and northward  
136 magnetic field in the magnetosheath were consistent with  
137 the solar wind conditions (Figure 1). The spacecraft  
138 entered back into the magnetosphere through the  
139 magnetopause on two more occasions, at the times  
140 indicated with vertical dashed lines. These re-entries  
141 correlate with drops in the solar wind density, observed as  
142 short periods of  $M_A \sim 2$  in Figure 1d.

143 The data that constitute the prime focus of the present  
144 paper is the ion-to-electron temperature ratio plotted in  
145 Figure 2d. It shows that  $T_i/T_e$  was unusually low in the  
146 magnetosheath. It was generally around 3, as compared to  
147 typical values being well above 6 in this region for high  
148  $M_A$  [Pashmann *et al.*, 1993; Phan *et al.*, 1994]. A short  
149 period of larger density around 6:20 UT, which  
150 corresponds to a slightly higher  $M_A$  ( $\sim 5$ -6 in Figure 1),  
151 shows a localised increase of  $T_i/T_e$  to about 5. [A second  
152 high  \$T\_i/T\_e\$  period is observed in the magnetosheath after  
153  \$\sim 13:10\$  UT, which appears related to particle leakage from  
154 the magnetopause.](#)

155 The key observation in Figure 2 is the low  $T_i/T_e$  in parts  
156 of the boundary layer intervals. Indeed, while fluctuations  
157 of  $T_i/T_e$  were measured during the wave activity of the  
158 first boundary layer encounter, and in part of the second,  
159 the ratio is essentially unchanged at  $\sim 3$  during the entire  
160 last boundary layer interval. This observation  
161 demonstrates that  $T_i/T_e$  in the boundary layers during low  
162  $M_A$  can be significantly lower than the typical values of  
163 either the magnetosheath or plasma sheet during high  $M_A$ .  
164 As discussed above, this boundary layer (centered at 12  
165 UT) corresponds to an effective  $M_A \sim 2$  in the solar wind  
166 (Figure 1d). The actual magnetosheath  $T_i/T_e$  was not  
167 measured at this time. It might have had a somewhat lower  
168  $T_i/T_e$  than during the observed magnetosheath intervals  
169 where  $T_i/T_e \sim 3$ , and which corresponded to  $M_A \sim 3$ -4.  
170 These observations yet demonstrate that  $T_i/T_e$  inside the  
171 magnetosphere can be anomalously low: whatever the  
172 plasma entry mechanism, it did not force this ratio to be  
173 high.

174 Wave activity, primarily seen in the magnetic field and  
175 flow (Figures 2e and 2f), was often detected in the  
176 magnetosheath. Wave activity in the magnetosheath was  
177 observed around 8 and 10 UT for instance, together with  
178 flow enhancements. No pronounced wave activity was  
179 seen inside the last two boundary layer intervals, contrary  
180 to the clear activity for the first magnetopause crossing.

181 The bottom panels of Figure 2 show a zoom of Cluster  
182 data for this crossing. Kelvin-Helmholtz (KH) waves are  
183 observed. The waves are characterized by typical anti-  
184 correlation between density and temperature (Figures 2h  
185 and 2i), and associated flow and magnetic field  
186 fluctuations (Figures 2e, 2f, and 2l). Periods with a  
187 substantial component of magnetospheric plasma, with  
188 low density but large temperatures (Figure 2i), were also  
189 observed (vertical dashed lines). Periods of boundary layer  
190 plasma, made of heated magnetosheath plasma inside the  
191 magnetopause, are highlighted with red arrows. The  
192 pristine cold magnetosheath was sampled towards the end  
193 of the interval.

194 Figure 2k shows that while  $T_i/T_e$  is high in the pre-  
195 existing magnetospheric plasma (vertical dashed lines), in  
196 the boundary layer (red arrows) it is of the order of that  
197 observed later in the pristine magnetosheath. As explained  
198 next, it is unclear whether the KH instability is the process  
199 that permitted plasma entry during this event. However, as  
200 for the case of the third boundary layer ( $\sim 12$  UT)  $T_i/T_e$  is  
201 significantly lower than usual at the times marked by red  
202 arrows in this boundary layer. The solar wind  $M_A$  is low  
203 and steady during this crossing (Figure 1d). Therefore,  
204  $T_i/T_e$  was essentially preserved upon entry through the  
205 magnetopause.

### 206 3. Discussion

207 The KH waves observed at the first magnetopause  
208 crossing on that day were nicely correlated with other  
209 spacecraft and ground observations of Pc5 waves in the  
210 magnetosphere, as demonstrated by *Rae et al.* [2005].  
211 They identified the Cluster KH observations between 2  
212 and 3 UT as the likely source of the Pc5 waves. For such  
213 low  $M_A$  conditions, the enhanced tailward flows observed  
214 at times in the magnetosheath (e.g.,  $\sim 3:30 - 4:00, 7:00 -$   
215  $8:30, 9:30 - 10:00$  UT) correspond to enhanced flows  
216 adjacent to the magnetopause in the fashion of a slingshot  
217 as described in previous works [*Chen et al.*, 1993;  
218 *Rosenqvist et al.*, 2007; *Lavraud et al.*, 2007]. As  
219 suggested by these authors, such enhanced flows may lead  
220 to stronger coupling through enhanced KH activity [cf.  
221 also *Lavraud and Borovsky*, 2008].

222 *Hasegawa et al.* [2006] recently devised a single-  
223 spacecraft method to discern KH waves that have entered  
224 a non-linear stage and are rolled-up. Using magneto-  
225 hydrodynamic simulations they showed that the low  
226 density plasma from the magnetospheric side is entrained  
227 in rolled-up vortices so as to lead to regions of low density  
228 (i.e., of magnetospheric origin) with tailward velocities  
229 larger than the dense magnetosheath itself. They tested  
230 and confirmed this property with spacecraft data (cf. also  
231 *Taylor et al.* [2008]). For the present KH wave  
232 observations, no clear such signature is found (not shown);  
233 it is thus not sure whether plasma entry was locally  
234 occurring owing to the KH activity.

235 Figures 2i – 2k show the total, parallel and  
236 perpendicular components of the ion and electron  
237 temperatures, as well as their ratios. Compatible with  
238 previous boundary layer observations for higher  $M_A$   
239 [*Hasegawa et al.*, 2003; *Nishino et al.*, 2007a], electrons  
240 show parallel temperature anisotropy in the boundary  
241 layers while ions are more isotropic. By contrast, ions

242 have a perpendicular anisotropy in the magnetosheath  
243 while electrons are more isotropic. This results in  
244 temperature ratios that follow similar trends for both  
245 components (Figure 2k), with the ratio of the  
246 perpendicular temperatures being higher than that for  
247 parallel temperatures. As noted by previous authors [e.g.,  
248 *Lee et al.*, 1994; *Johnson and Cheng*, 1997; *Nishino et al.*,  
249 2007b], these characteristics are possibly the result of  
250 wave-particle interactions upon entry through the  
251 magnetopause. However, *Taylor and Lavraud* [2008]  
252 recently found that boundary layer ions at times may be  
253 composed of two superposed cold populations of solar  
254 wind origin, each with different temperature anisotropy.  
255 The mechanisms that may explain the boundary layer  
256 anisotropy characteristics, and that would maintain the low  
257 temperature ratios as evidenced here, remain to be fully  
258 identified.

259 Finally, high  $T_i/T_e$  (above 10 or so) in Figure 2k marks  
260 the sampling of the plasma sheet. This high energy  
261 population was observed adjacent to and inside the  
262 boundary layers; it was seen as a single population on  
263 several occasions (vertical dashed lines). The high  $T_i/T_e$  of  
264 this population may indicate that it was formed at earlier  
265 times under higher  $M_A$  conditions; remember that  
266 *Baumjohann* [1993] found large scatter in  $T_i/T_e$  in the  
267 plasma sheet. This high value is also related to the  
268 spacecraft being located in the dusk-side magnetosphere.  
269 Indeed, high  $T_i/T_e$  is expected in the plasma sheet at dusk,  
270 and lower ones at dawn, owing to the differential gradient  
271 and curvature drifts of ions and electrons in the tail. That a  
272 significant high energy ion population exists at dusk more  
273 than at dawn has been clearly established in previous  
274 works [e.g., *Fujimoto et al.*, 1998; *Nishino et al.*, 2007a].  
275 Mixing of this high energy ion population with the newly  
276 entered cold plasma of solar wind origin is often observed,  
277 i.e., at times other than the vertical dashed lines and red  
278 arrows. [The short high  \$T\_i/T\_e\$  interval in the second  
279 boundary layer around 8:45 UT also seems related to  
280 mixing.](#) Such times correspond to intermediate values of  
281  $T_i/T_e$ , and can be explained by this mixing. This highlights  
282 the potential impact of transport processes, in addition to  
283 entry mechanisms.

## 284 5. Conclusions

285 We investigated the behavior of the ion-to-electron  
286 temperature ratio ( $T_i/T_e$ ) measured by Cluster in the dusk-  
287 side magnetosheath and magnetopause boundary layers for  
288 low solar wind Alfvén Mach number ( $M_A$ ), during the  
289 passage of a magnetic cloud at Earth. The observations  
290 showed  $T_i/T_e \sim 3$  in the magnetosheath, which is unusually  
291 low compared to typical values of order 6 – 12 for higher  
292  $M_A$ . This ratio is similarly low in the magnetopause  
293 boundary layers observed during this event. Thus,  
294 assuming that the plasma has recently entered these layers  
295 through the magnetopause, it has essentially preserved this  
296 property. It was not possible to determine with certainty  
297 which process formed these boundary layers, i.e.,  
298 reconnection, diffusion or KH instability. These  
299 observations demonstrate, at least for this event, that none  
300 of these entry mechanisms forced the temperature ratio to  
301 be high. This opens the possibility to distinguish which  
302 plasma entry mechanism prevails, e.g., if theoretical,

303 simulation and other observational works can shed light on  
304 how each mechanism may influence this ratio. No explicit  
305 temperature ratio predictions have been found for these  
306 mechanisms in previous works; but it is acknowledged  
307 that the literature is prolific on those subjects. In the  
308 future, this property may also be used to trace solar wind  
309 plasma transport into the inner regions of the  
310 magnetosphere, though keeping in mind that the ratio may  
311 evolve with transport in the tail owing in particular to the  
312 mixing of different populations in response to the  
313 differential drifts of ion and electron.

314  
315 **Acknowledgments.** The authors acknowledge the support of  
316 ISSI (Bern, Switzerland) for the organization of a combined  
317 Cluster-THEMIS study team. We are grateful for the use the  
318 AMDA/CDPP tool which allowed conditional searches of low  
319 Mach number intervals. We thank the OMNI data team for  
320 providing the solar wind data, as well as the ACE teams.

## 321 References

- 322  
323 Balogh, A., C. M. Carr, M. H. Acuña, et al. (2001), The Cluster  
324 magnetic field investigation: Overview of in-flight  
325 performance and initial results, *Ann. Geophys.*, 19(10-12),  
326 1207-1217.
- 327 Bame, S. J., J. R. Asbridge, J. T. Gosling, et al. (1979), High  
328 temporal resolution observations of electron heating at the  
329 bow shock, *Space Sci. Rev.*, 23, 75-92.
- 330 Baumjohann, W. (1993), The near-Earth plasma sheet: An  
331 AMPTE/IRM perspective, *Space Sci. Rev.*, 64, 141.
- 332 Chen, S.-H., M. G. Kivelson, J. T. Gosling, et al. (1993),  
333 Anomalous aspects of magnetosheath flow and of the shape  
334 and oscillations of the magnetopause during an interval of  
335 strongly northward interplanetary magnetic field, *J. Geophys.*  
336 *Res.*, 98(A4), 5727-5742.
- 337 Dungey, J. W. (1961), Interplanetary magnetic field and the  
338 auroral zones, *Phys. Rev. Lett.*, 6, 47.
- 339 Eastman, T. E., and E. W. Hones Jr. (1979), Characteristics of  
340 the magnetospheric boundary layer and magnetopause layer  
341 as observed by IMP 6, *J. Geophys. Res.*, 84(A5), 2019-2028.
- 342 Fujimoto, M., T. Terasawa, T. Mukai, et al. (1998), Plasma  
343 entry from the flanks of the near-Earth magnetotail: Geotail  
344 observations, *J. Geophys. Res.*, 103(A3), 4391-4408.
- 345 Génot, V., and S. J. Schwartz (2004), Spacecraft potential  
346 effects on electron moments derived from a perfect plasma  
347 detector, *Ann. Geophys.*, 22(6), 2073-2080.
- 348 Hasegawa, H., M. Fujimoto, K. Maezawa, Y. Saito, and T.  
349 Mukai (2003), Geotail observations of the dayside outer  
350 boundary region: Interplanetary magnetic field control and  
351 dawn-dusk asymmetry, *J. Geophys. Res.*, 108(A4), 1163,  
352 doi:10.1029/2002JA009667.
- 353 Hasegawa, H., M. Fujimoto, T. D. Phan, et al. (2004), Rolled-up  
354 Kelvin-Helmholtz vortices and associated solar wind entry at  
355 Earth's magnetopause, *Nature*, 430, 755-758.
- 356 Hasegawa, H., M. Fujimoto, K. Takagi, et al. (2006), Single-  
357 spacecraft detection of rolled-up Kelvin-Helmholtz vortices  
358 at the flank magnetopause, *J. Geophys. Res.*, 111, A09203,  
359 doi:10.1029/2006JA011728.
- 360 Johnson, J. R., and C. Z. Cheng (1997), Kinetic Alfvén waves  
361 and plasma transport at the magnetopause, *Geophys. Res.*  
362 *Lett.*, 24(11), 1423-1426.
- 363 Johnstone, A. D., C. Alsop, S. Burge, et al. (1997), PEACE: A  
364 plasma electron and current experiment, *Space Sci. Rev.*,  
365 79(1-2), 351-398.
- 366 Lavraud, B., M. F. Thomsen, B. Lefebvre, et al. (2006),  
367 Evidence for newly closed magnetosheath field lines at the  
368 dayside magnetopause under northward IMF, *J. Geophys.*  
369 *Res.*, 111, A05211, doi:10.1029/2005JA011266.
- 370 Lavraud, B., J. E. Borovsky, A. J. Ridley, et al. (2007), Strong  
371 bulk plasma acceleration in Earth's magnetosheath: A  
372 magnetic slingshot effect?, *Geophys. Res. Lett.*, 34, L14102,  
373 doi:10.1029/2007GL030024.

374 Lavraud, B., and J. E. Borovsky (2008), Altered solar wind-  
375 magnetosphere interaction at low Mach numbers: Coronal  
376 mass ejections, *J. Geophys. Res.*, 113, A00B08,  
377 doi:10.1029/2008JA013192.

378 Lee, L. C., J. R. Johnson, and Z. W. Ma (1994), Kinetic Alfvén  
379 waves as a source of plasma transport at the dayside  
380 magnetopause, *J. Geophys. Res.*, 99(A9), 17,405–17,411.

381 Mitchell, D., F. Kutchko, D. Williams, et al. (1987), An  
382 extended study of the low-latitude boundary layer on the  
383 dawn and dusk flank of the magnetosphere, *J. Geophys. Res.*,  
384 92(A7), 7394-7404.

385 Nishino, M. N., M. Fujimoto, T. Terasawa, G. Ueno, K.  
386 Maezawa, T. Mukai, and Y. Saito (2007a), Temperature  
387 anisotropies of electrons and two component protons in the  
388 dusk plasma sheet, *Ann. Geophys.*, 25(6), 1417-1432.

389 Nishino, M. N., M. Fujimoto, G. Ueno, T. Mukai, and Y. Saito  
390 (2007b), Origin of temperature anisotropies in the cold  
391 plasma sheet: Geotail observations around the Kelvin-  
392 Helmholtz vortices, *Ann. Geophys.*, 25(9), 2069-2086.

393 Nykyri, K., A. Otto, B. Lavraud, et al. (2006), Cluster  
394 observations of reconnection due to the Kelvin-Helmholtz  
395 instability at the dawnside magnetospheric flank, *Ann.*  
396 *Geophys.*, 24(10), 2619 – 2643.

397 Øieroset, M., J. Raeder, T. D. Phan, et al. (2005), Global cooling  
398 and densification of the plasma sheet during an extended  
399 period of purely northward IMF on October 22-24, 2003,  
400 *Geophys. Res. Lett.*, 32(12), L12S07,  
401 doi:10.1029/2004GL021523.

402 Paschmann, G., W. Baumjohann, N. Scopke, et al. (1993),  
403 Structure of the dayside magnetopause for low magnetic  
404 shear, *J. Geophys. Res.*, 98(A8), 13409-13422.

405 Phan, T. D., G. Paschmann, W. Baumjohann, et al. (1994), The  
406 magnetosheath region adjacent to the dayside magnetopause:  
407 AMPTE/IRM observations, *J. Geophys. Res.*, 99(A1), 121-  
408 141.

409 Rae, I. J., et al. (2005), Evolution and characteristics of global  
410 Pc5 ULF waves during a high solar wind speed interval, *J.*  
411 *Geophys. Res.*, 110, A12211, doi:10.1029/2005JA011007.

412 Rème, H., C. Aoustin, J. M. Bosqued, et al. (2001), First  
413 multispacecraft ion measurements in and near the Earth's  
414 magnetosphere with the identical CLUSTER Ion  
415 Spectrometry (CIS) Experiment, *Ann. Geophys.*, 19(10-12),  
416 1303-1354.

417 Rosenqvist, L., A. Kullen, and S. Buchert (2007), An unusual  
418 giant spiral arc in the polar cap region during the northward  
419 phase of a Coronal Mass Ejection, *Ann. Geophys.*, 25, 507-  
420 517.

421 Russell, C. T., M. M. Hoppe, W. A. Livesey, et al. (1982),  
422 ISEE-1 and -2 observations of laminar bow shocks: velocity  
423 and thickness, *Geophys. Res. Lett.*, 9(10), 1171–1174.

424 Schwartz, S. J., M. F. Thomsen, S. J. Bame, and J. Stansberry  
425 (1988), Electron heating and the potential jump across fast  
426 mode shocks, *J. Geophys. Res.*, 93(A11), 12,923–12,931.

427 Sibeck, D. G., G. Paschmann, R. A. Treumann, et al. (1999),  
428 Chapter 5 – Plasma transfer processes at the magnetopause,  
429 *Space Sci. Rev.*, 88, 207.

430 Song, P. and C. T. Russell (1992), Model of the formation of the  
431 low-latitude boundary layer for strongly northward  
432 interplanetary magnetic field, *J. Geophys. Res.*, 97(A2),  
433 1411-1420.

434 Taylor, M. G. G. T., B. Lavraud, C. P. Escoubet, et al. (2008),  
435 The plasma sheet and boundary layers under northward IMF:  
436 a multi-point and multi-instrument perspective, *Adv. Space.*  
437 *Res.*, 41(10), 1619-1629.

438 Taylor, M. G. G. T., and B. Lavraud (2008), Observation of  
439 three distinct ion populations at the Kelvin-Helmholtz-  
440 unstable magnetopause, *Ann. Geophys.*, 26(6), 1559-1566.

441 Terasawa, T., M. Fujimoto, T. Mukai, et al. (1997), Solar wind  
442 control of density and temperature in the near-Earth plasma  
443 sheet: WIND/GEOTAIL collaboration, *Geophys. Res. Lett.*,  
444 24(8), 935-938.

445 Thomsen, M. F., J. T. Gosling, S. J. Bame, et al. (1985), Ion and  
446 Electron Heating at Collisionless Shocks Near the Critical  
447 Mach Number, *J. Geophys. Res.*, 90(A1), 137–148.

448  
449



450 B. Lavraud, Centre d'Etude Spatiale des Rayonnements, 9  
451 Avenue du Colonel Roche, BP 44346, 31028 Toulouse Cedex 4,  
452 France. ([Benoit.Lavraud@cesr.fr](mailto:Benoit.Lavraud@cesr.fr))  
453

454 LAVRAUD ET AL.: TRACING SOLAR WIND PLASMA ENTRY

455

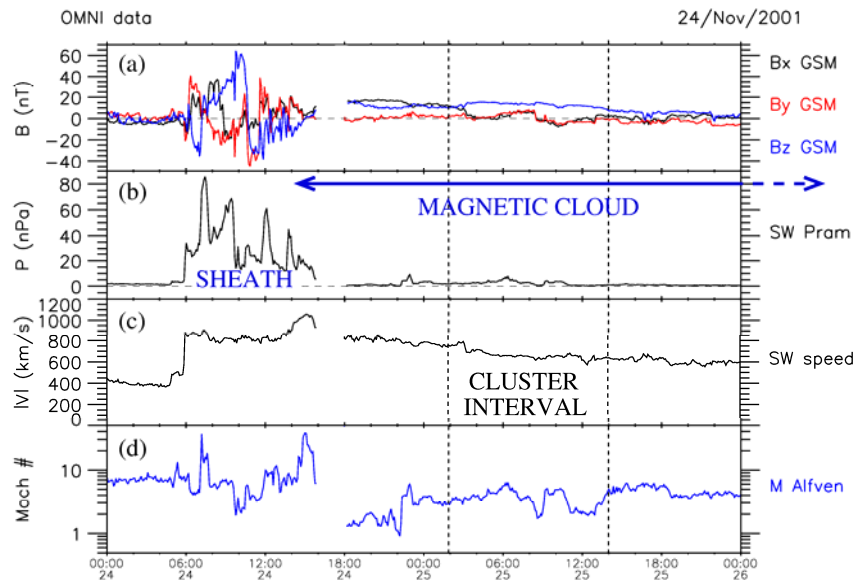
456

457

458 FIGURES:

459

460

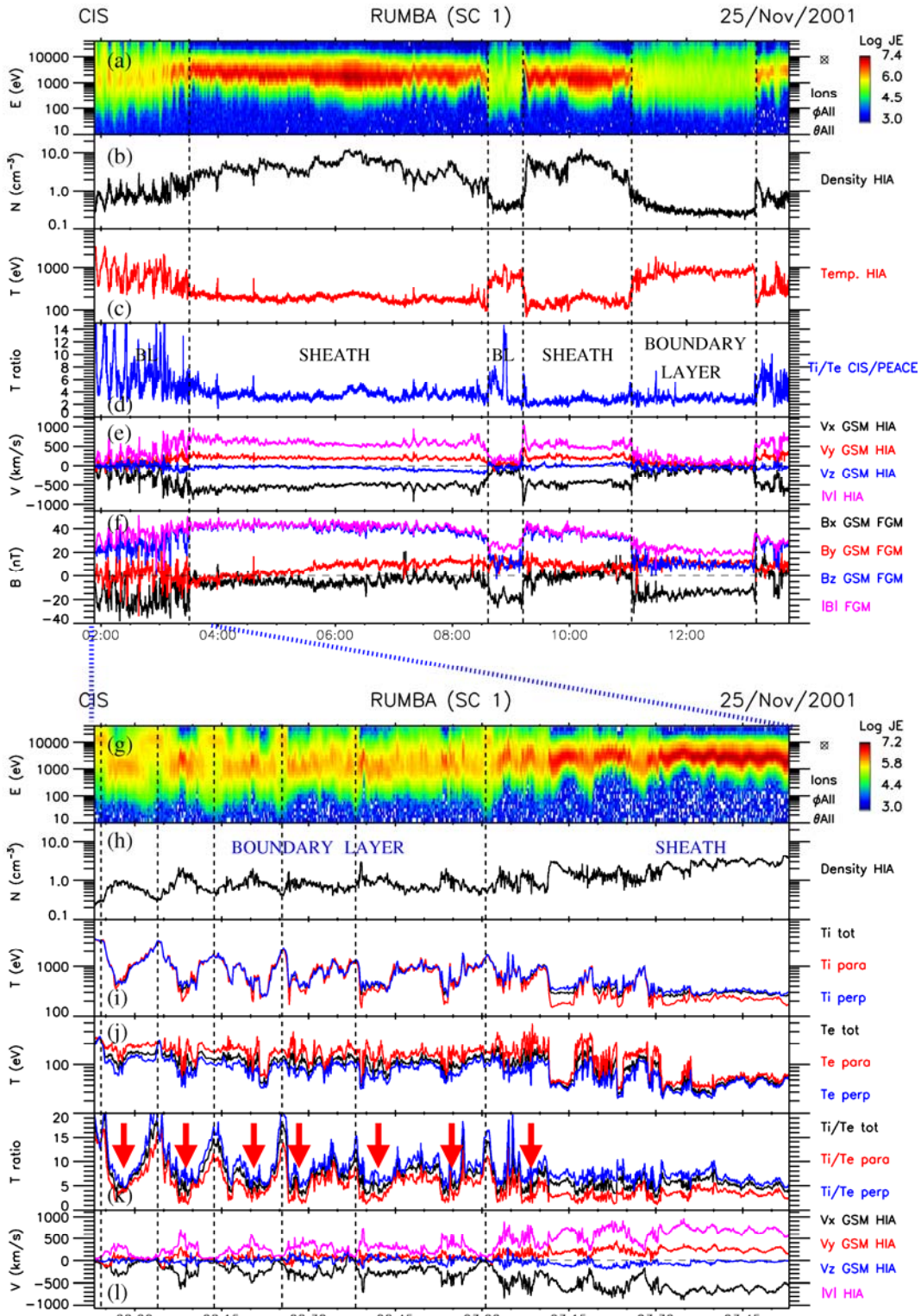


461

462 **Figure 1.** Interplanetary observations during the passage of a magnetic cloud at Earth on November 24 – 26, 2001. The  
463 panels show the solar wind (a) IMF components in GSM, (b) ram pressure, (c) speed, and (d) Alfvén Mach number.

464

465



466  
467  
468  
469  
470  
471  
472  
473  
474  
475

**Figure 2.** Cluster observations during the period of operation on November 25, 2001. The panels at the top show (a) the ion omnidirectional spectrogram (energy flux), (b) the total ion density, (c) the total ion temperature, (d) the ion-to-electron total temperature ratio, (e) the ion velocity components in GSM, and (f) the magnetic field components in GSM. Three boundary layer intervals were observed, with corresponding magnetopause crossings marked by vertical dashed lines. Panels (g) to (l) at the bottom show a zoom of Cluster data during the period of Kelvin-Helmholtz wave activity. Only the last four panels change. They display (i) the ion and (j) electron temperatures, (k) the ion-to-electron temperature ratios (all for total, parallel and perpendicular components), and (l) the ion velocity component. Times of enhanced  $T_i/T_e$  due to the appearance of a hot magnetospheric population are marked by vertical dashed lines. Times of clear boundary layer plasma with low  $T_i/T_e$ , similar to that of the magnetosheath are marked with red arrows in panel (k).